UNIVERSIDAD DE CHILE
FACULTAD DE CIENCIAS FÍSICAS Y MATEMÁTICAS
DEPARTAMENTO DE INGENIERÍA CIVIL

A MECHANISTIC MODEL FOR HYDROGEN PRODUCTION IN AN ANMBR TREATING HIGH STRENGTH WASTEWATER

TESIS PARA OPTAR AL GRADO DE MAGÍSTER EN CIENCIAS DE LA INGENIERÍA,
MENCIÓN RECURSOS Y MEDIO AMBIENTE HÍDRICO

GINO FRANCISCO VERA SÁNCHEZ

PROFESORA GUÍA
ANA LUCÍA PRIETO SANTA

MIEMBROS DE LA COMISIÓN:
FRANCISCO GRACIA CAROCA
CRISTIAN SALGADO HERRERA
RICARDO LUNA HERNÁNDEZ

Este trabajo ha sido financiado parcialmente por:
Proyecto Fondecyt número 11191123.

SANTIAGO DE CHILE
2024

RESUMEN DE LA TESIS PARA OPTAR
AL GRADO DE MAGÍSTER EN CIENCIAS DE LA INGENIERÍA,
MENCIÓN RECURSOS Y MEDIO AMBIENTE HÍDRICO
POR: GINO FRANCISCO VERA SÁNCHEZ
FECHA: 2024
PROF. GUÍA: ANA LUCÍA PRIETO SANTA

MODELO MECANÍSITICO PARA LA PRODUCCIÓN DE HIDRÓGENO EN UN REACTOR ANAERÓBICO DE MEMBRANA TRATANDO AGUA RESIDUAL DE ALTA CARGA

En este trabajo se desarrolla un modelo para la producción de hidrógeno en un reactor anaeróbico de membrana sumergida teniendo como sustrato aguas residuales multisustrato de alta carga. Los modelos existentes para simular reactores anaeróbicos de membranas tienen la desventaja de presentar monosustratos en la corriente afluente, lo que limita su utilización en sistemas complejos. La gran diferencia que presenta el modelo expuesto en este trabajo es que es capaz de simular la producción de hidrógeno a partir de la degradación de afluentes multisustratos, lo que se traduce en una extensión de los sistemas que pueden ser estudiados, ya sea en su diseño o en su optimización.

El objetivo general de este trabajo es el desarrollo de un modelo para la producción de hidrógeno en reactores anaeróbicos de membrana sumergida a partir de aguas residuales de alta carga. Para lograrlo, se formularon las ecuaciones que describen la fenomenología a partir de la fusión de modelos preexistentes que simularan la producción de hidrógeno en sistemas perfectamente agitados sin membrana, y de modelos que explicaran cómo la materia disuelta afecta en el desempeño de la membrana; la que a su vez influye directamente en los mecanimos ocurriendo dentro del reactor. Una vez formulado el modelo, y luego de obtener los resultados de la simulación, se hicieron comparaciones entre las predicciones y resultados experimentales reportados en literatura. Además, se realizó un análisis de sensibilidad, con el fin de obtener los parámetros críticos para producción de hidrógeno.

La simulación indica que la mayor producción de hidrógeno se logra con afluentes que poseen una mayor cantidad aminoácidos, seguida por la producción con afluentes ricos en azúcares y finalmente aquellos ricos en lípidos. Sin embargo, estos afluentes también están asociados a una mayor producción de EPS, lo que implica aumentar la frecuencia del lavado de la membrana.

Los casos extremos en la producción de hidrógeno corresponden a aquellos afluentes que poseen 100 % aminoácidos, y aquellos con una composición del 100 % ácidos grasos. Con una base de 10 g/L de materia orgánica en el afluente, se tiene una producción de 6,1 $L_{H_2}/L-d$ para el caso 100 % aminoácidos, con una frecuencia de retrolavado de 30 minutos; mientras que para el caso 100 % de ácidos grasos, se tiene una producción de 0,7 $L_{H_2}/L-d$, con una frecuencia de retrolavado de 60 minutos. Notar que todos los casos que corresponden a una combinación entre aminoácidos, azúcares y ácidos grasos se encuentran en los rangos mencionados.

Por otro lado, se tiene que el modelo es sensible a la temperatura, al tiempo de retención hidráulico y al tiempo de retención de sólidos. En este sentido, se tiene que la producción de hidrógeno se ve favorecida al operar en condiciones mesofílicas, con HRT en torno a las 12 horas y SRT en torno a los 6 días.

A MECHANISTIC MODEL FOR HYDROGEN PRODUCTION IN AN ANMBR TREATING HIGH STRENGTH WASTEWATER

In this work, a model was developed for hydrogen production in a submerged membrane anaerobic reactor with high-strength multisubstrate wastewater as substrate. Existing models for simulating membrane anaerobic reactors have the disadvantage of presenting monosubstrates in the influent stream, which limits their use in complex systems. The great difference presented by the model presented in this work is that it is capable of simulating hydrogen production from the degradation of multisubstrate influents, which results in an extension of the systems that can be studied, either in their design or in their optimization.

The overall objective of this work is the development of a model for hydrogen production in anaerobic submerged membrane reactors from high-load wastewater. To achieve this, the equations describing the phenomenology were formulated by merging pre-existing models that simulate hydrogen production in perfectly agitated systems without a membrane, and models that explain how dissolved matter affects membrane performance, which in turn directly influences the mechanisms occurring inside the reactor. Once the model was formulated, and after obtaining the simulation results, comparisons were made between the predictions and experimental results reported in the literature. In addition, a sensitivity analysis was performed to obtain the critical parameters for hydrogen production.

The simulation indicates that the highest hydrogen production is achieved with influents having a higher amount of amino acids, followed by production with sugar-rich influents and finally those rich in lipids. However, these influents are also associated with higher EPS production, which implies increasing the frequency of membrane washing.

The extreme cases in hydrogen production correspond to those influents with 100 % amino acids and those with 100 % fatty acid composition. With a base of 10 g/L of organic matter in the influent, there is a production of 6.1 $L_{H_2}/L-d$ for the case of 100 % amino acids, with a backwash frequency of 30 minutes; while for the case of 100 % fatty acids, there is a production of 0.7 $L_{H_2}/L-d$, with a backwash frequency of 60 minutes. Note that all the cases that correspond to a combination between amino acids, sugars, and fatty acids are in the mentioned ranges.

On the other hand, the model is sensitive to temperature, hydraulic retention time, and solids retention time. In this sense, hydrogen production is favored when operating under mesophilic conditions, with HRT around 12 hours and SRT around 6 days.

"Mientras tenga mi pasado conmigo,
puedo plantar ambos pies con más fuerza.
Si uno sabe quién es uno mismo, las dudas,
la vacilación y la ansiedad desaparecen."
Kimetsu No Yaiba

Agradecimientos

En primer lugar, quiero agradecer a mis padres por sacarse la cresta para que yo fuera capaz de estudiar. Sepan que los quiero mucho y que este logro también es de ustedes.

En segundo lugar, quiero agradecer a la profesora Ana Lucía Prieto, por ser una profesora guía tan seca y comprometida con mi formación. Guardo en mi corazón todos esos momentos que pasamos, ya sea durante la escritura del paper, la primera decepción de cuando nos rechazaron, las risas en ACS y todo. Muchas muchas gracias.

También quiero agradecer a todas las personas que me tiraban de las orejas para poder terminar este proceso. No fue un camino fácil, tuve altos y bajos que me llevaron a patear mucho esto, pero ya estamos ready jaja.

Finalmente, a mis amigos que estuvieron conmigo en todo este proceso. Muchas gracias por todos los consejos y todo el apoyo.

Finalmente, al Fondecyt número 11191123, por haber financiado parcialmente este trabajo de título.

Tabla de Contenido

Índice de Tablas

Índice de Ilustraciones

Capítulo 1

Introduction

Hydrogen has been recognized and established as an eco-friendly energy alternative, due to its oxidation has a high calorific value and presenting water as the only product (García-Depraect et al., 2019). Conventionally, hydrogen is produced by reforming hydrocarbons and alcohols, by hydrolysis of water or by thermochemical processes, however, these technologies have as a common denominator that they are not necessarily environmentally friendly because conventionally, the energy needed for the hydrogen production reactions to occur comes from non-renewable and/or fossil sources (Meher Kotay y Das, 2008).

Biohydrogen is a product of various chemical reactions carried out by microorganisms. Its production has attracted attention in recent years, due to the fact that it is eco-friendly since it allows revaluing waste and recovering energy simultaneously, in addition, it is positioned as a viable alternative to replace non-renewable energy sources (Rahman et al., 2016). Biohydrogen production can be carried out through different routes for sugar degradation, where the four main ones correspond to dark fermentation, photobiological, enzymatic and microbial electrolysis. Dark fermentation based processes have the advantage of not requiring aeration or a light source for H_2 production, facilitating their application in remote/decentralized areas where liquid wastes are available (Aziz et al., 2021).

In recent years, several waste-to-H2 technologies have been developed, among which anaerobic digestion in membrane bioreactors (AnMBR), biomass cogasification (Ramos y Silva, 2018) and water biophotolysis (Kapdan y Kargi, 2006) stand out. A novel technology for biohydrogen production corresponds to the Composite Bioactive Membrane (CBMem), which is composed of gas permeable microtubes that incorporate a liquid-gas separation, allowing hydrogen capture and removal during fermentation (Prieto et al., 2016). Hydrogen removal is beneficial for hydrogen production because the process is more favorable when the partial pressure of hydrogen decreases. However, for the technology to significantly favor gas production, it is necessary to control the growth of methanogenic bacteria, which consume hydrogen in their metabolism to produce methane; this is achieved by adequately controlling the operating conditions of the reactor (Hawkes et al., 2007).

Modeling becomes an essential tool for understanding the behavior of complex systems like AnMBRs for H_2 recovery (Boese-Cortés et al., 2023). A benchmark model to describe the biological stage in an AnMBR is the anaerobic digestion model 1 (ADM1) (Batstone et al., 2002), developed for the digestion of high-strength wastewater (concentration of COD over 1000 mg/L in the influent) (Shin et al., 2021). A modification to ADM1 was proposed by

Siegrist et al. (2002) (Siegrist et al., 2002), where mesophilic and thermophilic conditions were studied during digestion. The main limitation of both models is that they were designed only to predict the biochemical activity inside a reactor. However, a complete model of AnMBR must include additional processes that account for the presence of the membrane unit. For instance, membrane fouling represents one of the highest costs in the operation and maintenance of AnMBRs. Due to high concentrations of organic matter, extracellular polymeric substances (EPS) and soluble microbial products (SMP) play a crucial role in membrane fouling (Chen et al., 2017; Maaz et al., 2019). Some authors have modeled the membrane fouling mechanisms in a submerged AnMBR in response to the SMP and EPS concentrations (Gautam et al., 2022; Jang et al., 2006). The critical limitation of these models is the use of single substrates (e.g., hexoses), which might not represent actual wastewater and could lead to idealistic results in hydrogen generation. Additionally, these models might not be extrapolated to more complex systems.

Modeling treatment systems allows optimization of built systems, testing changes in operating conditions, and even designing new systems. This is why the development of a model that allows modeling a system that treats not only ideal monosubstrate aqueous effluents, but also a system that treats real effluents with high organic load appears to be necessary. Figure 1.1 establishes the expected relationship between the biochemical and physical models. The biochemical model explains the main forms of biomass decay, specifically the fermentation of amino acids and sugars, the oxidation of long chain fatty acids (LCFA), the decay of microorganisms, among others; while the physical model tries to explain how the accumulation of biomass inside the reactor affects the transmembrane pressure that must be applied, and how to reduce fouling in the membrane.

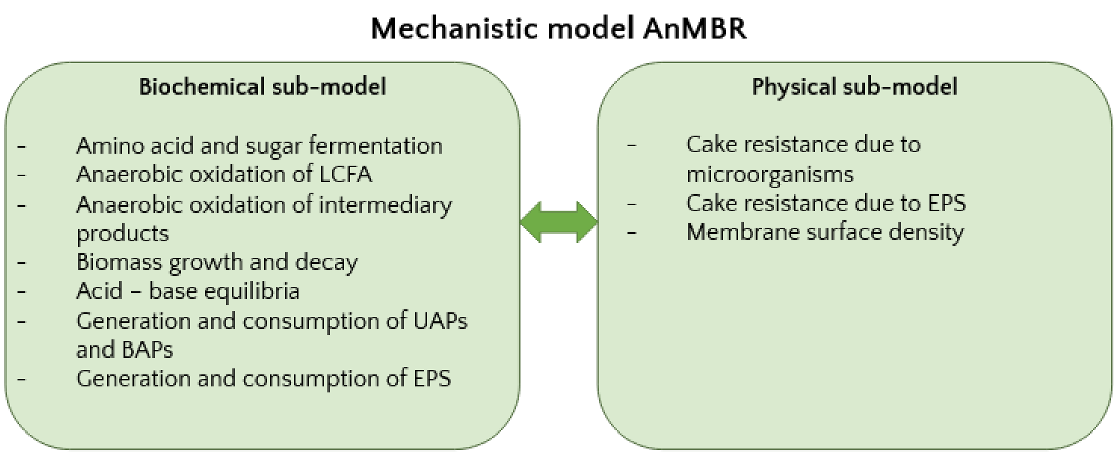

Figura 1.1: Interaction between biochemical model and physical model.

The main objective of this thesis is to develop a mechanistic model for hydrogen production in submerged AnMBR treating high-strength wastewater. The model builds on the ADM1 model and incorporates physical and biochemical processes to describe membrane fouling due to a multi-substrate influent (i.e., carbohydrates, proteins, and fats) and their impact on hydrogen production. Additionally, a sensitivity analysis establishes the key operating conditions of the system for H2 production. The study aims to provide a useful tool that accurately represents the physical and biochemical processes occurring in a submerged AnMBR treating a multi-substrate influent, to aid the design and simulation of the operation of this system for H2 recovery in high-strength waste streams.

Objectives

Development of a hydrogen production model in a submerged membrane reactor to treat high load wastewater.
The specific objectives (S.O.) and the tasks for each S.O. are described as follows:

- (S. O. 1) Formulate a phenomenological model of the system (AnMBR-CBMems).

  1. (T1) Define the process line based on a bibliographic review.
  2. (T2) Define the organic matter transformation processes that will be considered for modeling.
  3. (T3) Select models that adapt to the process line and that include the processes defined in T2. Formulate the mass balances for each of the species present in the digestion based on the ADM1 model (Batstone et al., 2002) and the Anaerobic Sewae Sludge Digestion model (Siegrist et al., 2002). Incorporate the fouling process, related to the membrane, into the model.

- (S. O. 2) Study the sensitivity of the model in different operational conditions in order to determine critical parameters of the operation.

  1. (T4) Perform a sensitivity analysis with the “one parameter at a time” technique.
  2. (T5) Graphically compare the evolution of the output variables in response to the fluctuation of the operational parameters.
  3. (T6) Graphically compare the evolution of the output variables with the change in the compositions of the organic matter fed to the reactor.
  4. (T7) Determine the frequency at which the membrane should be cleaned to reduce the fouling phenomenon.

- (S. O. 3) Compare the results of the model with results obtained in literature.

  1. (T8) Select studies that have similar operating conditions to establish comparisons of results.
  2. (T9) Test operating conditions from reported studies to compare model output with experimental results.

Thesis Outline

The main product of this thesis is one scientific article, included in Chapter 2. The article presents the methodology to obtain the hydrogen production model, the final model, the behaviour of the different studied variables, and the sensitivity of the model to disturbances (Vera, Feijoo, y Prieto, 2023) (graphical abstract in Figure 1.2).

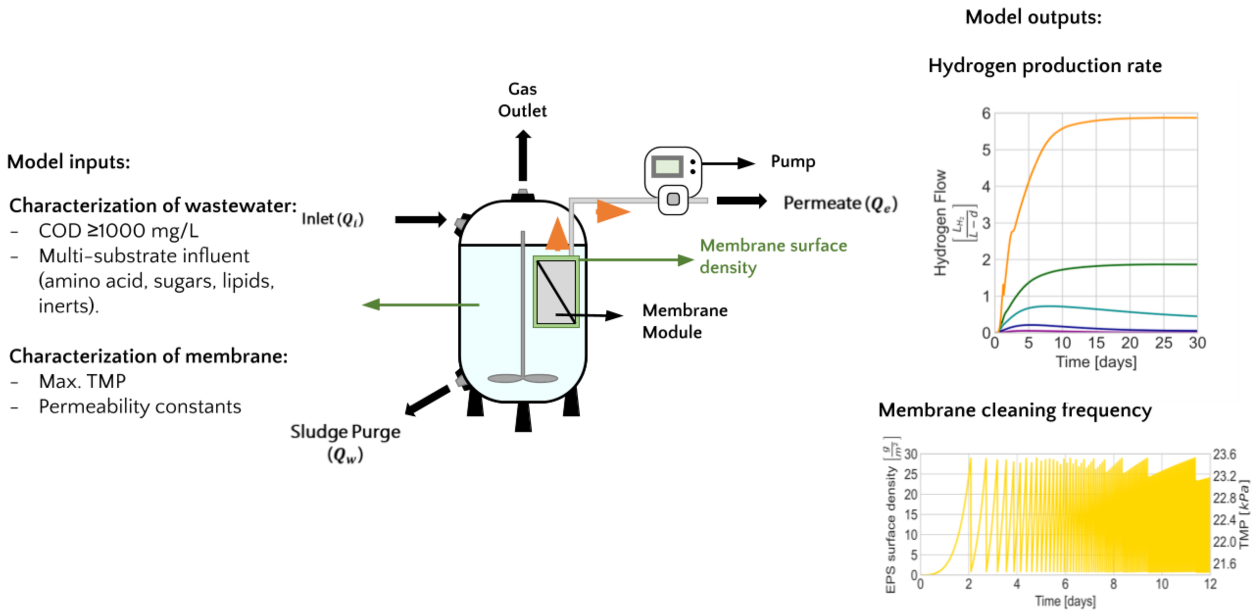

Figura 1.2: Graphical abstract of the mechanistic model with its inputs and outputs.

Capítulo 2

Modelo mecanístico para la producción de hidrógeno en un reactor anaeróbico de membrana tratando agua residual de alta carga

Autores:
Gino Vera, Felipe A. Feijoo, Ana L. Prieto

Palabras clave:
Modelo AnMBR; modelo multisustrato; fouling de membrana; hidrógeno de fermentación; agua residual a H_2

RESUMEN

En la carrera mundial por producir hidrógeno verde, la conversión de aguas residuales en H_2 es una alternativa sostenible que sigue sin explotar. Las tecnologías eficientes para convertir aguas residuales en H_2 aún se encuentran en sus etapas de desarrollo y se requiere urgentemente una intensificación del proceso. En nuestro estudio, se desarrolló un modelo mecanicista para caracterizar la producción de hidrógeno en un AnMBR que trata aguas residuales de alta carga (DQO $>$ 1000 mg/L). Dos aspectos diferencian nuestro modelo de la literatura existente: primero, la entrada del modelo es un agua residual de múltiples sustratos que incluye fracciones de proteínas, carbohidratos y lípidos. En segundo lugar, el modelo integra el modelo ADM1 con procesos físicos/bioquímicos que afectan el rendimiento de la membrana (por ejemplo, fouling la membrana). El modelo incluye balances de masa de 27 variables en estado transiente, donde se incluyeron metabolitos, sustancias poliméricas extracelulares, productos microbianos solubles y densidad superficial de la membrana. Los resultados del modelo mostraron que la tasa de producción de hidrógeno era mayor cuando se trataban afluentes ricos en azúcar y aminoácidos, lo que está fuertemente relacionado con una mayor generación de EPS durante la digestión de estos metabolitos. La tasa más alta de producción de H_2 para afluentes ricos en aminoácidos fue de 6,1 $\frac{L_{H2}}{L-d}$; para afluentes ricos en azúcar fue de 5,9 $\frac{L_{H2}}{L-d}$; y para afluentes ricos en lípidos fue de 0,7 $\frac{L_{H2}}{L-d}$. Los ciclos de lavado y fouling de membrana modelados mostraron comportamientos extremos para sustratos ricos en aminoácidos y ácidos grasos. Nuestro modelo ayuda a identificar limitaciones operativas para la producción de H_2 en AnMBR, proporcionando una herramienta valiosa para el diseño de sistemas MBR fermentativos/anaeróbicos orientados hacia la recuperación de energía.

A Mechanistic Model for Hydrogen Production in an AnMBR Treating High Strength Wastewater

Membranes
https://doi.org/10.3390/membranes13110852

Authors:
Gino Vera, Felipe A. Feijoo, Ana L. Prieto

Keywords:
AnMBR model; multi-substrate model; membrane fouling; fermentative hydrogen; wastewater-to-H_2

ABSTRACT:
In the global race to produce green hydrogen, wastewater-to-H_2 is a sustainable alternative that remains unexploited. Efficient technologies for wastewater-to-H_2 are still in their developmental stages, and urgent process intensification is required. In our study, a mechanistic model was developed to characterize hydrogen production in an AnMBR treating high-strength wastewater (COD > 1000 mg/L). Two aspects differentiate our model from existing literature: First, the model input is a multi-substrate wastewater that includes fractions of proteins, carbohydrates, and lipids. Second, the model integrates the ADM1 model with physical/biochemical processes that affect membrane performance (e.g., membrane fouling). The model includes mass balances of 27 variables in a transient state, where metabolites, extracellular polymeric substances, soluble microbial products, and surface membrane density were included. Model results showed the hydrogen production rate was higher when treating amino acids and sugar-rich influents, which is strongly related to higher EPS generation during the digestion of these metabolites. The highest H_2 production rate for amino acid-rich influents was 6.1 LH_2/L-d; for sugar-rich influents was 5.9 LH_2/L-d; and for lipid-rich influents was 0.7 LH_2/L-d. Modeled membrane fouling and backwashing cycles showed extreme behaviors for amino- and fatty-acid-rich substrates. Our model helps to identify operational constraints for H_2 production in AnMBRs, providing a valuable tool for the design of fermentative/anaerobic MBR systems toward energy recovery.

2.1. Introduction

Among the existing technologies for biochemical waste-to-H_2 production, including microbial fuel cells, microbial electrolysis cells, algae-catalyzed processes (biophotolysis and photofermentation), and even gas-separation MBR [1,2], those based on dark fermentation have the advantage of not requiring aeration or a light source for H_2 production, facilitating their application in remote/decentralized areas where liquid wastes are available [3]. Many of these technologies, however, are still in their developmental stages, and urgent process intensification is required to cope with the growing demand for renewable hydrogen. Anaerobic membrane bioreactors (AnMBRs) are mature technologies traditionally used to decrease COD concentrations in high-strength waste streams [4,5]. However, this treatment objective has now switched to a more sustainable approach, where valuable resources such as nutrients, energy, and water can be recovered [6]. Depending on the reactor operation, AnMBRs can produce methane and/or hydrogen while generating high-quality effluents for further wastewater reclamation [7,8]. Several studies report their application for H_2 recovery using non-competing feedstocks, such as food waste, agricultural residual waste (e.g., winery or sugar beet), animal-generated waste (e.g., dairy), organic fraction of municipal solid waste, or wastewater, among others [7,9–13]. However, information about biohydrogen production in AnMBRs is still limited to lab and pilot scales due to the stringent control of operational variables, the need for substrate pre-treatment, energy cost, membrane fouling, H_2 stripping, OLR maintenance, or even microbial competition [14].

Modeling becomes an essential tool for understanding the behavior of complex systems like AnMBRs for H_2 recovery [1]. A benchmark model to describe the biological stage in an AnMBR is the anaerobic digestion model 1 (ADM1) [15], developed for the digestion of high-strength wastewater (concentration of COD over 1000 mg/L in the influent) [16]. A modification to ADM1 was proposed by Siegrist et al. (2002) [17], where mesophilic and thermophilic conditions were studied during digestion. The main limitation of both models is that they were designed only to predict the biochemical activity inside a reactor. However, a complete model of AnMBR must include additional processes that account for the presence of the membrane unit. For instance, membrane fouling represents one of the highest costs in the operation and maintenance of AnMBRs. Due to high concentrations of organic matter, extracellular polymeric substances (EPS) and soluble microbial products (SMP) play a crucial role in membrane fouling [18,19]. Some authors have modeled the membrane fouling mechanisms in a submerged AnMBR in response to the SMP and EPS concentrations [20,21]. The critical limitation of these models is the use of single substrates (e.g., hexoses), which might not represent actual wastewater and could lead to idealistic results in hydrogen generation. Additionally, these models might not be extrapolated to more complex systems. Recent advances in AnMBR modeling include numerical and statistical techniques like machine/deep learning. However, reproducibility is problematic for these models since they are limited to the system where the data were collected [22–24]. A summary of the main model structures in the literature used for modeling AnMBR is shown in Table 2.1. Modeling structures often do not include biochemical and physical processes together, except those modeling membrane cake fouling due to EPS and SMP, which are limited to one substrate and focus on the EPS [21,25].

Tabla 2.1: Summary of modeling structures for AnMBR in the literature. These include reactor configuration, biochemical and physical processes, and treatment objectives.

Model	Reactor Type	Biochemical Processes	Membrane Processes	Objective	Source
ADM 1	CSTR	Hydrolysis of carbohydrates, proteins, lipids. Uptake of sugars, amino acids, LCFA, butyrate, propionate, acetate, and hydrogen. Growth and decay of microorganisms.	NA	Describe the anaerobic digestion, quantifying the degradation and consumption of macronutrients, monomers, gases and biomass.	[15]
First order dynamic model	Not specific	Degradation of VS	NA	To be an easy tool to predict biogas generation.	[26]
Modified Gompertz model	Batch biogass reactor	Production of biogas	NA	Describe biogas generation from a non-linear regression obtained from empirical observations.	[27]
Artificial Neural Networks	Not specific	Not specific	Not specific	Predict the behavior of systems based on collected empiric data from them.	[26,28]
Membrane cake fouling model due to EPS	SAnMBR	Substrate degradation Growth and decay of microorganisms. Production of EPS.	Membrane fouling, Transmembrane pressure.	Elucidate the membrane fouling due to EPS in SAnMBR and its impact in membrane durability.	[21,25]

In this study, we developed a mechanistic model for hydrogen production in submerged AnMBR treating high-strength wastewater. The model builds on the ADM1 model and incorporates physical and biochemical processes to describe membrane fouling due to a multi-substrate influent (i.e., carbohydrates, proteins, and fats) and their impact on hydrogen production. Additionally, a sensitivity analysis established the key operating conditions of the system for H_2 production. The study aims to provide a useful tool that accurately represents the physical and biochemical processes occurring in a submerged An- MBR treating a multi-substrate influent, to aid the design and simulation of the operation of this system for H_2 recovery in high-strength waste streams.

2.2. Materials and methods

2.2.1. AnMBR Setup and Operational Conditions

The modeled system consists of a continuous stirred tank reactor (CSRT) coupled to a submerged liquid-separation membrane. Figure 2.1 shows a schematic of the system, including the inlet flow (Q_{in}), gas outlet, sludge purge (Q_w), and permeate flow (Q_e). Although the modeled processes were temperature- and pH-dependent, initial conditions were 35 ^{o}C and pH 7. Other parameters included inlet microbial concentration, COD concentration, and substrate composition (amino acids, sugars, long-chain fatty acids, and inert matter content). Initial values were 50 mg/L of microorganisms in the feed and a COD inlet of 4000 mg/L, as established by Siegrist et al., 2002 [17]. The reactor volume (V) was 1 m^3 and the hydraulic retention time (HRT) was 12 h. For hydrogen production in AnMBRs, there is no standard value for solids retention time (SRT) in the current literature [29,30]. Thus, we selected a conservative SRT of 6 days as a starting point since some studies suggest SRT values higher than 15 days might decline H_2 production rates [31]. Permeate flux was defined by $Q_e =$

V/HRT, and the sludge purge flux was defined as $Q_w = V/SRT$.

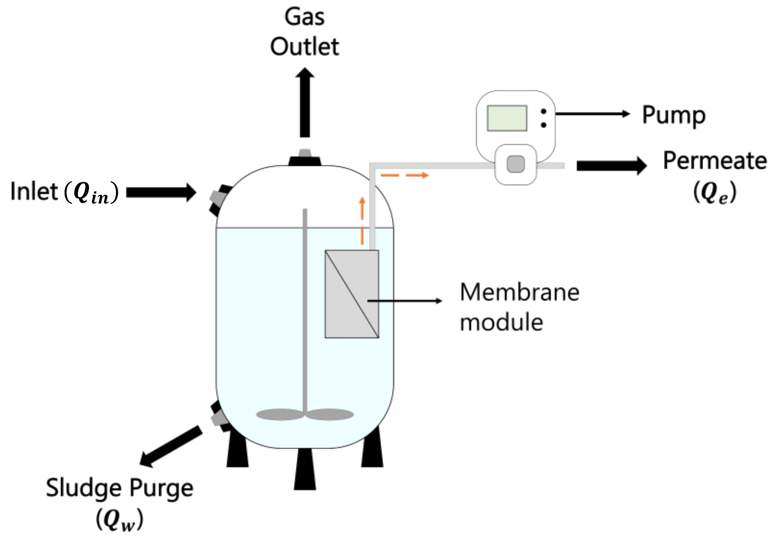

Figura 2.1: Schematic of the modeled system.

2.2.2. Modeling hydrogen production

The mass balances for the soluble compounds involved in the AnMBR model are shown in Equation (1).

$$V\frac{dS_i}{dt} = Q_{in}S_i^{in} - Q_eS_i^e - Q_wS_i^w + r_iV \tag{1}$$

where S_i corresponds to the concentration of a soluble specie i.
The mass balance for particulate compounds, microorganisms included, is shown in Equation (2). Complete retention by the membrane is assumed for particulate compounds.

$$V\frac{dX_i}{dt} = Q_{in}X_i^{in} - Q_wX_i^w + r_iV \tag{2}$$

where X_i corresponds to the concentration of a particulate specie i.
The rates of the processes (rows) involved in the consumption or generation of each compound inside the reactor (columns) are summarized in the Peterson Matrix and calculated with Equation (3).

$$r_i = \sum_i^{26}\sum_j^{20}\nu_{j,i}\rho_j \tag{3}$$

where r_i is the kinetic reaction rate law for a compound i, $\nu_{j,i}$ is a stoichiometric coefficient, and ρ_j is the kinetic expression for a process j.

2.2.2.1. Bioreactor Model Kinetics

The anaerobic digestion model includes the hydrolysis of particulate organic matter, fermentation and oxidation of metabolites, biomass growth and decay, and production and consumption of soluble microbial products (SMP) and extracellular polymeric substances (EPS). The processes involved in this model are described as follows.

- Degradation of particulate organic matter ρ_1: Particulate matter is composed by macronutrients and dead biomass, which are hydrolyzed into amino acids, sugars, and long chain fatty acids (LCFA). This process is described in Equation (4).

$$\rho_1 = k_H X_S \tag{4}$$

  where k_H is the hydrolysis constant rate, and X_S is the concentration of the total substrate.

- Fermentation of amino acids ρ_2 and sugars ρ_3: both processes were based on the Michaelis–Menten (MM) model (Equations (5) and (6)) and inhibited by pH.

$$\rho_2 = \mu_{max,2} \frac{S_{aa}}{K_{S,aa} + S_{aa}} I_{pH,2} X_{aa} \tag{5}$$

$$\rho_3 = \mu_{max,3} \frac{S_{su}}{K_{S,su} + S_{su}} I_{pH,2} X_{su} \tag{6}$$

  where $\mu_{max,2}$ and $\mu_{max,3}$ are the maximum growth rates for fermentation, S_{aa} and S_{su} are the concentrations of amino acids and sugars, respectively; $K_{S,aa}$ and $K_{S,su}$ are the half-saturation constants; and X_{aa} and X_{Su} are the concentration of amino acids and sugar degraders.

- Anaerobic oxidation of LCFA ρ_4: this process also follows a MM model; however, it presents inhibition due to acetate concentration, hydrogen concentration, and pH (Equation (7)).

$$\rho_4 = \mu_{max,4} \frac{S_{fa}}{K_{S,fa} + S_{fa}} I_{ac,4} I_{H_2,4} I_{pH,4} X_{fa} \tag{7}$$

  where $\mu_{max,4}$ is the maximum growth rate for anaerobic oxidation, S_{fa} is the concentration of long chain fatty acids, $K_{s,fa}$ is the half-saturation constant for LCFA, and X_{fa} is the concentration of LCFA degraders.

- Anaerobic oxidation of intermediary products ρ_5: for propionate, the expression for oxidation is given by Equation (8), following the MM model. This process is inhibited by acetate, hydrogen, pH level and ammonia concentration.

$$\rho_5 = \mu_{max,5} \frac{S_{pro}}{K_{S,pro} + S_{pro}} I_{ac,5} I_{H_2,5} I_{pH,6} I_{NH_3} X_{pro} \tag{8}$$

  where $\mu_{max,5}$ is the maximum growth rate for oxidation, S_{pro} is the concentration of propionate, $K_{S,fa}$ is the half-saturation constant for propionate, and X_{pro} is the concentration of propionate degraders.

- Acetotrophic methanogenesis ρ_6: based on the MM model and inhibited by pH level and ammonia concentrations.

$$\rho_6 = \mu_{max,6} \frac{S_{ac}}{K_{S,ac} + S_{ac}} I_{pH,6} I_{NH_3} X_{ac} \tag{9}$$

where $\mu_{max,6}$ is the maximum growth rate, S_{ac} is the concentration of acetate, $K_{S,ac}$ is the half-saturation constant for acetate, and X_{ac} is the concentration of acetate degraders.

- Hydrogenotrophic methanogenesis ρ_7: based on the MM model and inhibited by ammonia and hydrogen concentrations (Equation (10)).

$$\rho_7 = \mu_{max,7} \frac{S_{H_2}}{K_{S,H_2} + S_{H_2}} I_{pH,6} I_{NH_3} X_{H_2} \tag{10}$$

where $\mu_{max,7}$ is the maximum growth rate, S_{H_2} is the concentration of hydrogen, K_{S,H_2} is the half-saturation constant for hydrogen, and X_{H_2} is the concentration of hydrogen degraders.

- Biomass decay ρ_8–ρ_{13}: first order kinetics was assumed for decay (Equation (11)).

$$\rho_j = k_{d,j} X_i \tag{11}$$

where $k_{d,j}$ is the kinetic decay constant, and X_i is the concentration of a specific microorganism.

- Bicarbonate and dissolved carbon dioxide equilibrium ρ_{14}: described in Equation (12), the kinetic expression is based on the equilibrium Equation (13).

$$\rho_{14} = k_{eq,CO_2/HCO_3^-} \left(S_{HCO_3^-} S_{H^+} - S_{CO_2} K_{CO_2/HCO_3^-} \right) \tag{12}$$

$$CO_2 + H_2O \leftrightarrow HCO_3^- + H^+ \tag{13}$$

where $k_{eq,CO_2/HCO_3^-}$ is the rate constant for carbon dioxide/carbonate equilibrium, K_{CO_2/HCO_3^-} is the equilibrium constant for carbon dioxide/carbonate system. $S_{HCO_3^-}$ is the concentration of the ion bicarbonate, S_{H^+} is the concentration of protons, and S_{CO_2} is the concentration of carbon dioxide.

- Ammonia and ammonium equilibrium ρ_{15}: described in Equation (14), the kinetic expression is based on the equilibrium Equation (15).

$$\rho_{15} = k_{eq,NH_4^+/NH_3} \left(S_{NH_3} S_{CO_2} - \frac{S_{NH_4^+} S_{HCO_3^-} K_{NH_4^+/NH_3}}{K_{CO_2/HCO_3^-}} \right) \tag{14}$$

$$NH_4^+ + HCO_3^- \leftrightarrow NH_3 + CO_2 + H_2O \tag{15}$$

where $k_{eq,NH_4^+/NH_3}$ is the rate constant for ammonia/ammonium equilibrium, $K_{NH_4^+/NH_3}$ is the equilibrium constant for ammonia/ammonium system, $S_{NH_4^+}$ is the concentration of ion ammonium, and S_{NH_3} is the concentration of ammonia.

- Acetate and propionate protonation ρ_{16}–ρ_{17}: two pseudo equilibrium processes were considered (Equations (16) and (17)).

$$\rho_{16} = k_{eq,hac/ac} \left(S_{ac} S_{CO_2} - \frac{S_{hac} S_{HCO_3^-} K_{hac/ac}}{K_{CO_2/HCO_3^-}} \right) \tag{16}$$

where $k_{eq,,hac/ac}$ is the rate constant for acetic acid/acetate equilibrium, $K_{hac/ac}$ is the equilibrium constant for acetic acid/acetate system, S_{hac} is the concentration of the acetic acid, and S_{ac} is the concentration of acetate.

$$\rho_{17} = k_{eq,hpro/pro}\ (S_{ac}S_{CO_2} - \frac{S_{hpro}S_{HCO_3^-}K_{hpro/pro}}{K_{CO_2/HCO_3^-}}) \tag{17}$$

where $k_{eq,hpro/pro}$ is the rate constant for propionic acid/propionate equilibrium, $K_{hpro/pro}$ is the equilibrium constant for propionic acid/propionate system, S_{hpro} is the concentration of the propionic acid, and S_{pro} is the concentration of propionate.

- Inhibition processes: the following non-competitive inhibition expressions were considered.

$$I_{ac,j} = \frac{K_{I,ac,j}}{K_{I,ac,j} + S_{ac}} \tag{18}$$

$$I_{H_2,j} = \frac{K_{I,H_2,j}}{K_{I,H_2,j} + S_{H_2}} \tag{19}$$

$$I_{NH_3,j} = \frac{K^2_{I,NH_3,j}}{K^2_{I,NH_3,j} + S^2_{NH_3}} \tag{20}$$

$$I_{pH,j} \ = \frac{K^2_{I,NH_3,j}}{K^2_{I,NH_3,j} + S^2_{H^+}} \tag{21}$$

where $K_{I,ac,j}$, $K_{I,H_2,j}$, $K^2_{I,NH_3,j}$, and $K^2_{I,NH_3,j}$ are the inhibition constants for acetate, hydrogen, ammonia, and pH, respectively; S_{H_2} is the concentration of hydrogen, S_{NH_3} is the concentration of ammonia, and S_{H^+} is the concentration of protons.

- Temperature dependency: expressed by Equation (22).

$$\gamma = \gamma_{35^\circ C} \cdot \exp\left(\theta \cdot (T - 35)\right) \tag{22}$$

where $\gamma_{35^\circ\mathrm{C}}$ is the value of a parameter at 35 °C, θ is the corrector parameter, and T is the objective temperature. Parameters with temperature dependency are shown in Table 2.2.

2.2.2.2. Membrane Model Kinetics

The membrane model depends on biological processes that include the hydrolysis of EPSs to BAPs, formation of BAPs and UAPs in proportion to the substrate utilization, and biodegradation of BAPs and UAPs. The formation of BAPs, UAPs, and EPSs from a multi-substrate is one of the main attributes of the current study since these processes are often modeled to consider a single substrate. The model does not account for membrane sparging, pH, temperature control, and fluid dynamics inside the tank. The kinetic parameters related to the mentioned processes are described as follows.

- BAP and UAP decay ρ_{18}–ρ_{19}: these processes were modeled following the expression developed by Jang et al., 2006 [20], which established MM mechanisms for the decay, as shown in Equations (23) and (24).

$$\rho_{18} = k_{d,BAP} \frac{S_{BAP}}{K_{S,BAP} + S_{BAP}} X_a \tag{23}$$

$$\rho_{19} = k_{d,UAP} \frac{S_{UAP}}{K_{S,UAP} + S_{UAP}} X_a \tag{24}$$

where $k_{d,BAP}$ and $k_{d,UAP}$ are the maximum specific substrate utilization rates for BAP and UAP, $K_{S,BAP}$ and $K_{S,UAP}$ are the half-saturation constants for BAP and UAP, S_{BAP} and S_{UAP} are the BAP and UAP concentration, and X_a is the active biomass ($\sum_i^n X_i$).

- EPS decay ρ_{20}: first order kinetics was assumed for this process (Equation (25)).

$$\rho_{20} = k_2 S_{EPS} \tag{25}$$

where k_2 is the BAP formation rate coefficient, and S_{EPS} is the concentration of EPS.

- Fouling model: The accumulation of EPS density on the membrane surface (m) can be expressed as shown in Equation (26).

$$\frac{dm}{dt} = J S_{EPS} - k_{dm} m \tag{26}$$

where J is the flux through the membrane, and k_{dm} is the detachment rate of the EPS from the membrane (Equation (27)).

$$k_{dm} = \eta \left(\tau_m - \Delta_m \Delta P\right) \tag{27}$$

where η is a constant, τ_m is the shear stress, Δ_m is the static friction coefficient, and ΔP is the transmembrane pressure. In addition, the flux can be expressed as

$$J = \frac{\Delta P}{\mu \left(\alpha_s m + R_m\right)} \tag{28}$$

where μ is the dynamic viscosity of the permeate, α_s is the specific resistance of EPS, and R_m is the membrane resistance.

Finally, backwashing frequency (BW) was set according to Yoon (2005) [32] for a membrane filtration performance under recommended operational conditions (transmembrane pressure should not exceed 30 kPa).

2.2.2.3. Liquid–Gas Mass Transfer

Mass transfer from the liquid to the gas phase was modeled according to Equation (29).

$$F_j = -k_j (S_{j,interface} - S_j) \tag{29}$$

where k_j is the mass transfer coefficient for analyte j, $S_{j,interface}$ is the concentration of j in the interface, and S_j is the concentration of the analyte j in the liquid bulk.

$S_{j,interface}$ was estimated according to Equation (30).

$$S_{j,interface} = \frac{p_j}{H_j \exp\left(\theta_{Henry} T\right)} \tag{30}$$

where p_j is the partial pressure of j in the gas section, H_j is the Henry's constant for j, θ_{Henry} is a temperature correction factor, and T is the operation temperature. Partial pressure p_j was estimated using the ideal gases law.

Tabla 2.2: Parameters used in the model.

Parameter	**Value**	**Units**	$\theta(^oC^{-1})$	**Reference**
k_H	0.25	d^{-1}	0.024	[17]
$\mu_{max,2}$	4	d^{-1}	0.069	
$\mu_{max,3}$	4	d^{-1}	0.069	
$\mu_{max,4}$	0.6	d^{-1}	0.055	
$\mu_{max,5}$	0.6	d^{-1}	0.055	
$\mu_{max,6}$	0.37	d^{-1}	0.069	
$\mu_{max,7}$	2	d^{-1}	0.069	
$k_{d,8}$	0.8	d^{-1}	0.069	
$k_{d,9}$	0.8	d^{-1}	0.069	
$k_{d,10}$	0.06	d^{-1}	0.055	
$k_{d,11}$	0.06	d^{-1}	0.055	
$k_{d,12}$	0.05	d^{-1}	0.069	
$k_{d,13}$	0.3	d^{-1}	0.069	
$k_{d,BAP}$	0.07	$\frac{mg_{BAP}}{mg_{X_a}-d}$	-	[20]
$k_{d,UAP}$	0.4	$\frac{mg_{UAP}}{mg_{X_a}-d}$	-	
$k_{S,aa}$	50	$\frac{mg}{L}$	0.069	[17]
$k_{S,su}$	50	$\frac{mg}{L}$	0.069	
$k_{S,fa}$	1000	$\frac{mg}{L}$	0.035	
$k_{S,pro}$	20	$\frac{mg}{L}$	0.10	
$k_{S,ac}$	40	$\frac{mg}{L}$	0.10	
$k_{S,h2}$	1	$\frac{mg}{L}$	0.08	
$K_{S,BAP}$	85	$\frac{mg}{L}$	-	[20]
$K_{S,UAP}$	100	$\frac{mg}{L}$	-	
k_{eqCO2/HCO_3^-}	10	$\frac{m^3}{mol-d}$	-	[17]
$k_{eqNH_4^+/NH_3}$	10	$\frac{m^3}{g-d}$	-	
$k_{eqhac/ac}$	10	$\frac{m^3}{g-d}$	-0.004	
$k_{eqhpro/pro}$	10	$\frac{m^3}{g-d}$	-0.004	
K_{CO_2/HCO_3^-}	$7.1 \cdot 10^{-4}$	$\frac{mol}{m^3}$	0.004	
$K_{NH_4^+/NH_3}$	10^{-6}	$\frac{mol}{m^3}$	0.063	

Tabla 2.2: Parameters used in the model (continued).

Parameter	Value	Units	$\theta(^oC^{-1})$	Reference
$K_{hac/ac}$	0.025	$\frac{mol}{m^3}$	-	[17]
$K_{hpro/pro}$	0.019	$\frac{mol}{m^3}$	-	
$K_{I,ac,4-5}$	1500	$\frac{mg}{L}$	-	
$K_{I,H_2,4}$	3	$\frac{\mu g}{L}$	0.08	
$K_{I,H_2,5}$	1	$\frac{\mu g}{L}$	0.08	
$K_{I,pH,2-3}$	0.01	$\frac{mol}{m^3}$	-	
$K_{I,pH,4-7}$	$5 \cdot 10^{-4}$	$\frac{mol}{m^3}$	-	
$K_{I,NH_3,5}$	25	$\frac{mg}{L}$	0.061	
$K_{I,NH_3,6}$	17	$\frac{mg}{L}$	0.086	
k_1	0.05	$\frac{mg_{UAP}}{mg_S}$	-	[20]
k_2	0.02	$\frac{mg_{BAP}}{mg_{EPS}-d}$	-	
η	0.1	$\frac{1}{Pa-d}$	-	[25]
τ_m	5	Pa	-	[33]
Δ_m	10^{-3}	-	-	[25]
μ	0.0013	$Pa - s$	-	[21]
a_s	$5 \cdot 10^{12}$	$\frac{m}{kg}$	-	
R_m	$1.45 \cdot 10^{12}$	m^{-1}	-	
H_{H_2}	58	-	-0.002	[17]
H_{CO_2}	1.65	-	0.017	

2.2.3. Model parameters and numerical techniques

The parameters used for the model solution are summarized in Table 2.2. For this study, a transient state for a CSTR was assumed. The developed model was solved using ode15s with non-negative condition from MATLAB (The MathWorks Inc., Natick, MA, USA). To check for the stability of the model, the model's steady state as a function of the initial conditions was evaluated. The model was set to an inlet total substrate concentration of 10.000 $\frac{mg_{COD}}{L}$, and the following initial conditions: (a) $MLSS > 0$, $COD_{initial} = 0\frac{mg_{COD}}{L}$; (b) $MLSS = 0$, $COD_{initial} = 0\frac{mg_{COD}}{L}$; (c) $MLSS > 0$, $COD_{initial} = 5000\frac{mg_{COD}}{L}$; (d) $MLSS > 0$, $COD_{initial} = 10.000\frac{mg_{COD}}{L}$.

2.2.4. Model response and sensitivity analysis

To analyze the response of the model to changes in the inlet concentration and composition, we evaluated influent/inlet configurations presented in Table 2.4. Additionally, we evaluated the same inlet configurations, along with variable backwashing protocols, to observe the response of the EPS membrane surface density and the transmembrane pressure (TMP). For the sensitivity analysis, critical parameters affecting the hydrogen production were determined by using the one-factor-at-a-time (OAT) technique. We varied the kinetic and the operational parameters (SRT, HRT, and temperature) by ±50 % to identify their impact on the hydrogen production.

Tabla 2.3: Peterson Matrix

Units	**mol-m^3**	**mgCOD-m^3**	**g-m^3**	**mol-m^3**	**mol-m^3**	**g-m^3**	**g-m^3**	**gCOD-m^3**	**gCOD-m^3**	**gCOD-m^3**	**gCOD-m^3**	**gCOD-m^3**	**gCOD-m^3**
n° component	1	2	3	4	5	6	7	8	9	10	11	12	13
Process	S_{H^+}	S_{H_2}	S_{CH_4}	S_{CO_2}	$S_{HCO_3^-}$	$S_{NH_4^+}$	S_{NH_3}	S_{ac}	S_{hac}	S_{pro}	S_{hpro}	S_{aa}	S_{su}
ρ_1				0.0004	-0.0005							0.30	0.2
ρ_2		0.96		0.043	-0.022	0.587		3.29		1.42		-6.67	
ρ_3		0.96		0.091	-0.07	-0.08		3.29		1.42			-6.67
ρ_4		6.70		0.199	-0.202	-0.08		14.3					
ρ_5		8.20		0.162	0.004	-0.08		10.8		-20			
ρ_6			39.0	-0.006	0.618	-0.08		-40.0					
ρ_7		-22.0	21.0	-0.353	-0.006	-0.08							
ρ_8					0.003	0.045							
ρ_9					0.003	0.045							
ρ_{10}					0.003	0.045							
ρ_{11}					0.003	0.045							
ρ_{12}					0.003	0.045							
ρ_{13}					0.003	0.045							
ρ_{14}	-1			1	-1								
ρ_{15}				-1	1	14.0	-14.0						
ρ_{16}				-1	1			-64.0	64				
ρ_{17}				-1	1					-112	112		
ρ_{18}													
ρ_{19}													
ρ_{20}													

Tabla 2.3: Peterson Matrix (continued).

Units	**mol-m^3**	**mgCOD-m^3**	**g-m^3**	**mol-m^3**	**mol-m^3**	**g-m^3**	**g-m^3**	**gCOD-m^3**	**gCOD-m^3**	**gCOD-m^3**	**gCOD-m^3**	**gCOD-m^3**	**gCOD-m^3**
n° component	14	15	16	17	18	19	20	21	22	23	24	25	26
Process	S_{fa}	S_{in}	X_S	X_{aa}	X_{su}	X_{fa}	X_{pro}	X_{ac}	X_{H_2}	X_{in}	S_{BAP}	S_{UAP}	S_{EPS}
ρ_1	0.45	0.05	-1										
ρ_2				1-k_{EPS}-k_1								k_1	k_{EPS}
ρ_3					1-k_{EPS}-k_1							k_1	k_{EPS}
ρ_4	-22.0					1-k_{EPS}-k_1						k_1	k_{EPS}
ρ_5							1-k_{EPS}-k_1					k_1	k_{EPS}
ρ_6								1-k_{EPS}-k_1				k_1	k_{EPS}
ρ_7									1-k_{EPS}-k_1			k_1	k_{EPS}
ρ_8			0.8	-1						0.2			
ρ_9			0.8		-1					0.2			
ρ_{10}			0.8			-1				0.2			
ρ_{11}			0.8				-1			0.2			
ρ_{12}			0.8					-1		0.2			
ρ_{13}			0.8						-1	0.2			
ρ_{14}													
ρ_{15}													
ρ_{16}													
ρ_{17}													
ρ_{18}				$Y_p f_{aa}$	$Y_p f_{su}$	$Y_p f_{fa}$	$Y_p f_{pro}$	$Y_p f_{ac}$	$Y_p f_{h2}$		-1		
ρ_{19}				$Y_p f_{aa}$	$Y_p f_{su}$	$Y_p f_{fa}$	$Y_p f_{pro}$	$Y_p f_{ac}$	$Y_p f_{h2}$			-1	
ρ_{20}											1		-1

Tabla 2.4: Inlet variable composition to evaluate model response.

Case	COD (mg/L)	%Amino Acids	%Sugars	%Fatty Acids	%Inner Matter
A	2000				
B	4000				
C	7000				
D	10000				
E	20000				
1		100	0	0	0
2		0	100	0	0
3		0	0	100	0
4		30	20	45	5
5		30	45	20	5
6		31.3	46.3	21.3	0
7		30	45	20	5
8		31.66	31.66	31.66	5
9		31.66	21.66	46.66	0

2.3. Results and Discussion

2.3.1. Steady State Analysis

Figure 2.2 shows the results of different paths to the steady state from different initial conditions. The simulation indicates that the steady state for the substrate, biomass concentration, and hydrogen flow remains constant for all the tested conditions. At low COD initial concentrations, the curves remain smooth. However, once the reactor is fed (transient state), noise begins to appear in the curves as the concentration increases (Figure 2.2 c,d). The explanation for this phenomenon lies in the expressions of generation and consumption of each of the metabolites. The algebraic expressions for generation and/or consumption directly depend on the metabolites' concentration. As a result, irregularities in the curves could be due to high derivative values. This behavior is typical for ADM1 and ADM1-based models, as an overprediction of the metabolites' concentrations is often reported under start-up conditions [17]. For design and scale-up purposes, it is essential to consider steady-state conditions.

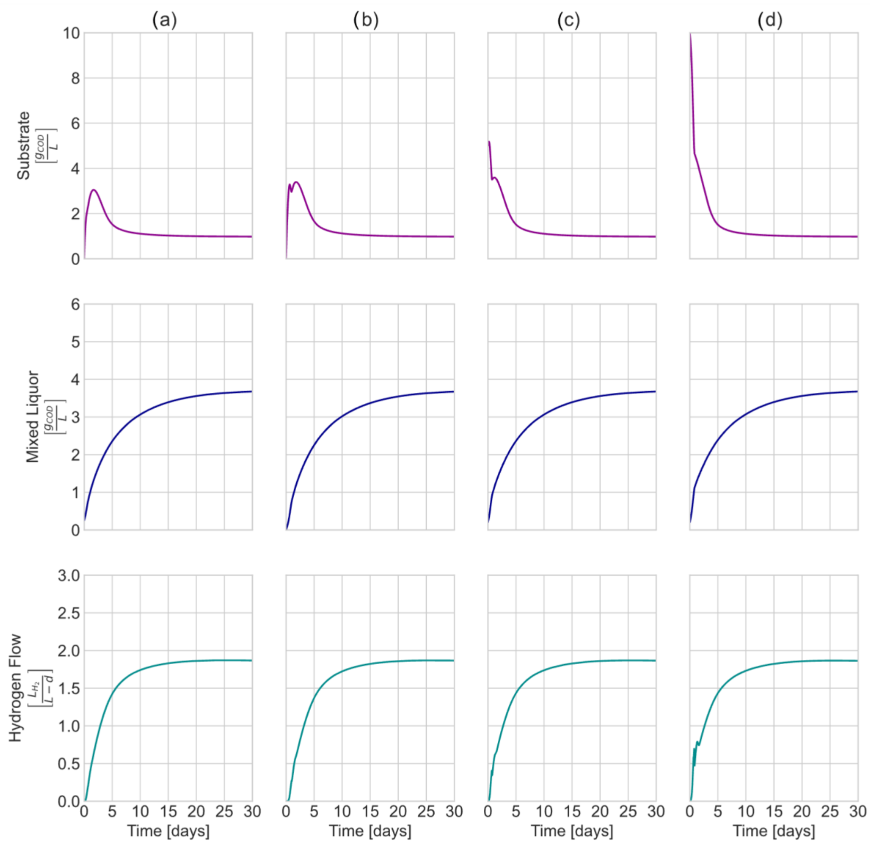

Figura 2.2: Evaluation of different steady states due to changes in initial conditions. For all four simulations, CODinlet = 10,000 mgCOD/L. (a) Biomass inside the reactor > 0, CODinitial = 0. (b) Biomass inside the reactor = 0, CODinitial = 0. (c) Biomass inside the reactor > 0, CODinitial = 5000 mgCOD/L. (d) Biomass inside the reactor > 0, CODinitial = 10,000 mgCOD/L.

2.3.2. AnMBR model behavior at Variable CODinlet and substrate composition

Figure 2.3 illustrates the simulation results for the evolution of biomass, EPS, and hydrogen, considering different values of inlet COD with a multi-substrate composition of 30 % amino acids, 20 % sugars, 45 % fatty acids, and 5 % inert matter [17]. The chosen COD values are representative of high-strength wastewater, as described by Shin et al. (2021) [16]. The simulation exhibited the expected behavior for each set of CODinlet concentrations, showing increasing biomass, EPS, and hydrogen production with higher CODinlet. However, the biogas composition depended on the substrate composition. Specifically, when considering a 10 g/L CODinlet with variable content of amino acids/sugars/fatty acids/inert matter, the largest hydrogen production was observed with a 100 % amino acids substrate (Case 1). However, this substrate composition also generated the highest EPS concentrations in the mixed liquor, potentially impacting membrane durability and performance [34,35].

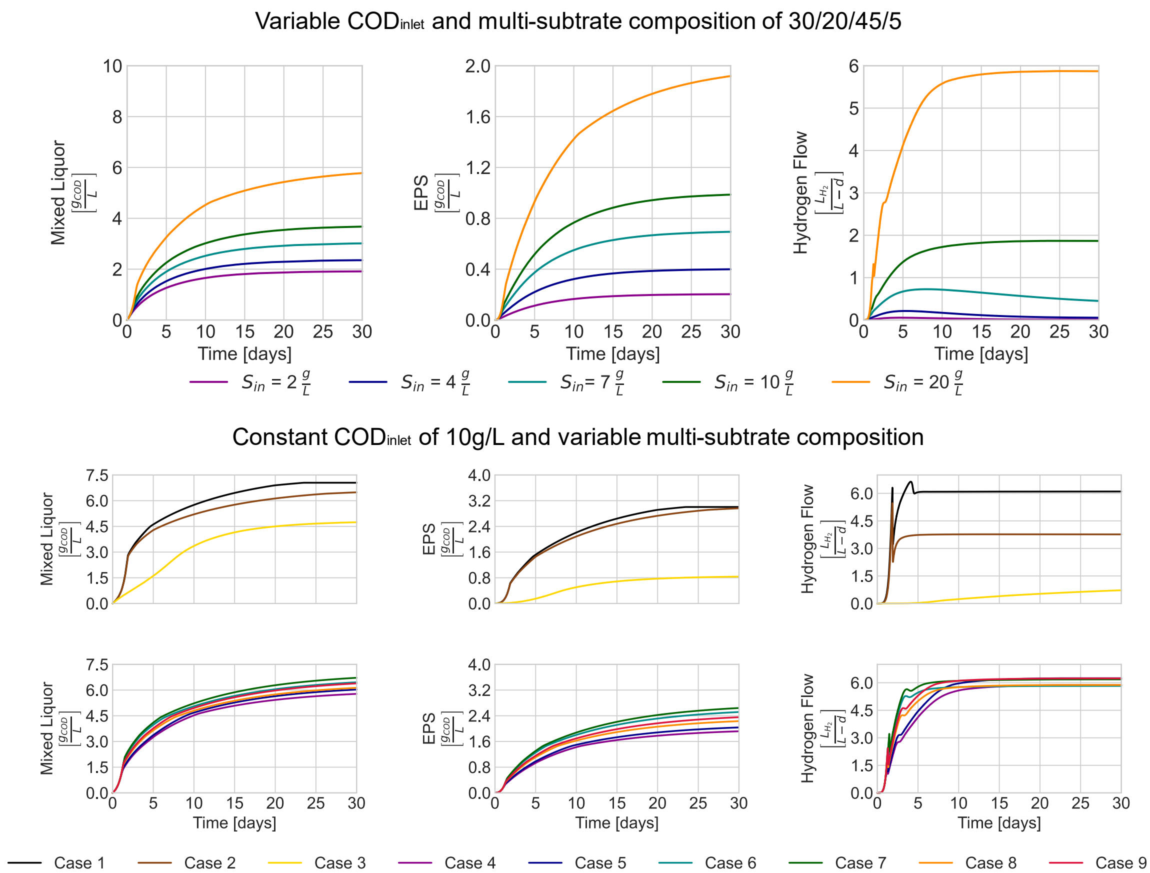

Figura 2.3: Modeled biomass, EPS, and hydrogen output for variable COD and multi-substrate composition (amino-acids/sugars/fatty-acids/inert-matter). Case 1— 100/0/0/0, Case 2—0/100/0/0, Case 3—0/0/100/0, Case 4—30/20/45/5, Case 5—30/45/20/5, Case 6—31.3/46.3/21.3/0, Case 7—30/45/20/5, Case 8—31.66 /31.66/31.66/5, Case 9—31.66/21.66/46.66/0.

Stoichiometrically, hydrogen production should be higher with a 100 % sugar substrate (Case 2). However, the results indicated possible inhibition in H_2 production from propionate oxidation due to carbon dioxide accumulation (Equation (17)). When considering a hypothetical waste stream composed solely of fatty acids, biomass growth was lower compared to those with 100 % content of amino acids or sugars (Cases 1 and 2). Hydrogen production and EPS were also limited, mainly because fatty acids were not involved in propionate generation, one of the start-up metabolites in the modeled hydrogen production. Additionally, LCFA kinetics were slower compared to sugars and amino acids. Overall, the results of the simulations suggest an enhanced hydrogen production in the AnMBR when treating multi-substrate influents rather than single-substrate ones.

Regarding membrane operation, Figure 2.4 illustrates the fouling control cycles for cases 1 and 3. Backwashing occurs when the transmembrane pressure reaches a value 10 % higher than the initial pressure (m = 0, Equation (20)). This restriction leads to an EPS surface density close to 30 g/m2. Figure 2.5 focuses on cases 1 and 3, representing the extremes of all the simulated cases. Influent with higher fatty acid concentrations results in less EPS production and, consequently, less frequent backwashing. Conversely, influents with a higher amino acid content (Figure 2.4, Case 1) require more membrane fouling control, leading to more frequent backwashing. To further analyze the data, Table 2.5 summarizes the number of events and backwashing frequency for different influent compositions. The number of backwashing events for all the evaluated cases tends to stabilize after four SRTs or 24 days from the start of operation once the EPS concentration reaches a steady state. Generally, influents with higher content of sugars and amino acids require more frequent backwashing events due to their strong relationship with EPS generation.

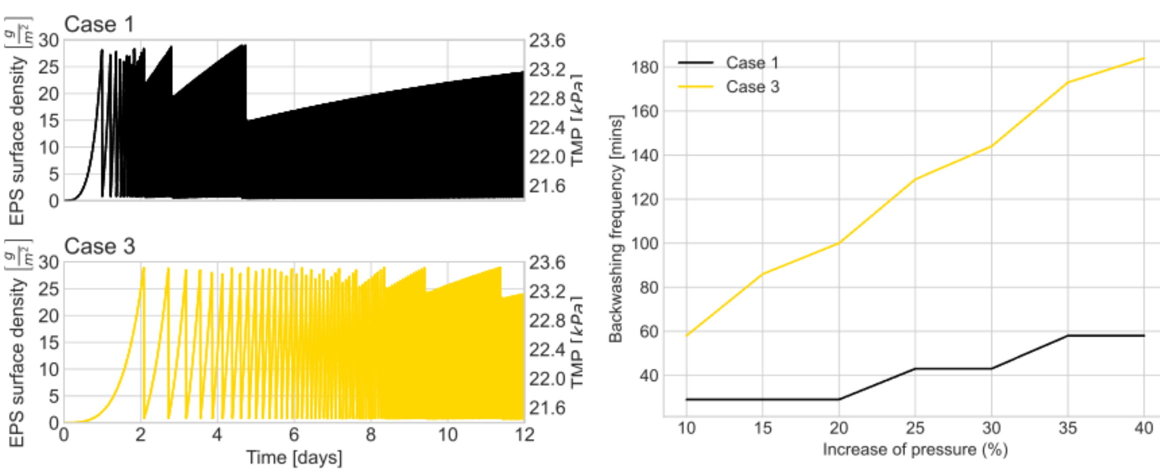

Figura 2.4: Left: Effect of inlet composition in EPS surface density and TMP. Time series follows the same trend for both EPS and TMP. Right: Effect of increasing transmembrane pressure tolerance in backwashing frequency. Case 1—100/0/0/0, Case 3—0/0/100/0.

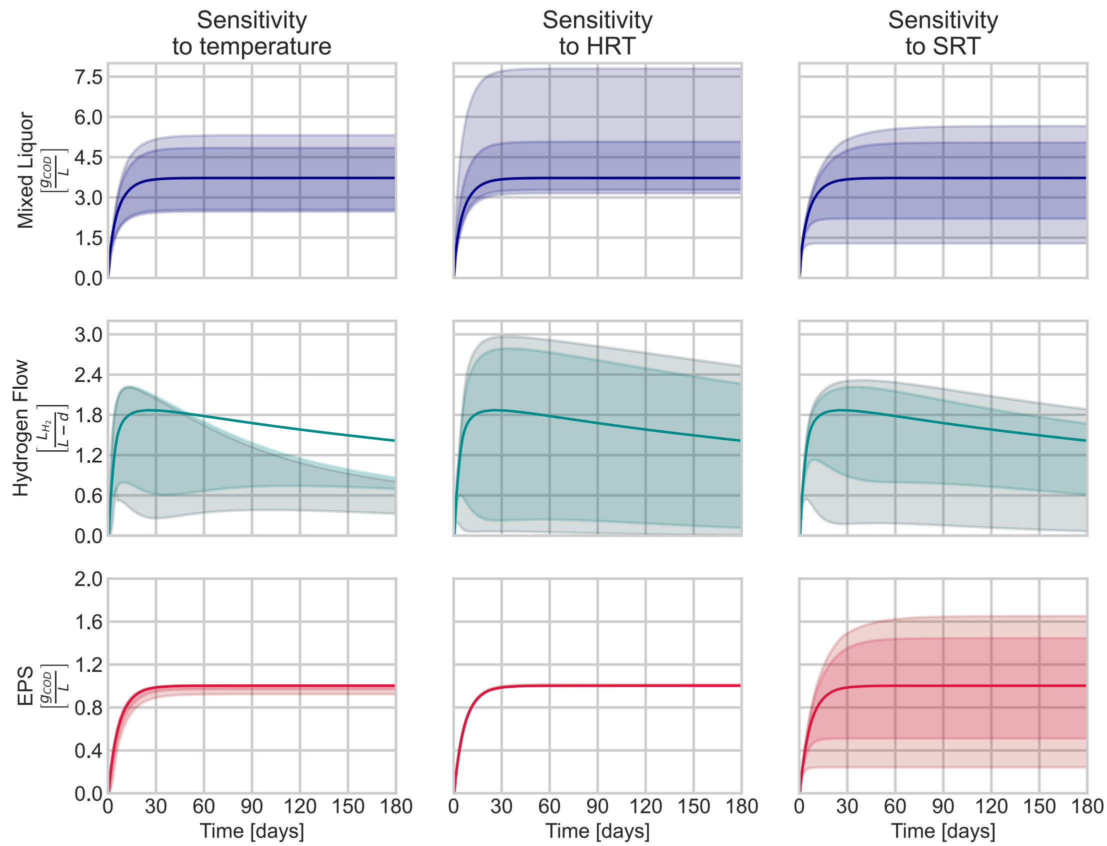

Figura 2.5: Changes in concentration of MLSS, biohydrogen production rate, and EPS concentration in relation to temperature, HRT, SRT. This simulation was obtained for HRT of 12 h, SRT of 6 d, inlet COD of 10 g/L, and a temperature of 35 ^{o}C. The figure shows an OAT analysis for variations of 50 % (darkest) and 70 % (lighter) for the mentioned design variables.

Tabla 2.5: Effect of inlet composition in the backwashing frequency (HRT 12 h).

SRT (6d)	**N^o of SRT since start of operation**					**Min. Average Frecuency**	**Max. Average Frecuency**
	1	**2**	**3**	**4**	**5**		
Case	(0-6) d	(6-12) d	(12-18) d	(18-24) d	(24-30) d	Min	Min
1	160	301	301	301	301	54	29
2	153	301	301	301	301	56	29
3	16	85	128	150	150	540	58
4	107	224	300	300	300	81	29
5	113	242	300	300	300	76	29
6	134	292	301	301	301	64	29
7	137	300	300	300	300	63	29
8	125	271	301	301	301	69	29
9	128	281	300	300	300	68	29

It is important to highlight that the backwashing frequency also changes as a function of the transmembrane pressure restrictions (Figure 2.4). As expected, backwashing is less frequent when the transmembrane pressure tolerance is higher. Since there is not an optimal value set in the current literature, then the condition for backwashing must be set according to the user's design and operational criteria (e.g., membrane lifetime, energy efficiency, etc.) [36,37]. When TMP is allowed to increase, the membrane is overstressed, which could reduce its lifespan [38]. On the contrary, more frequent backwashing cycles might extend the membrane's life, resulting in higher energy demand due to pumping.

2.3.3. Sensitivity analysis

Figure 2.5 presents the results of the OAT analysis for three variables that notably impact hydrogen production and membrane fouling. Temperature changes ($\pm 50\,\%$ change) directly affect the kinetic expressions governing mixed liquor solids (i.e., biomass) and hydrogen flow. The OAT analysis reveals that the temperature should be maintained under mesophilic conditions to increase hydrogen production, as there is no significant advantage observed with thermophilic operation. Higher temperatures increase hydrogen solubility, promoting inhibition (Equations (18)–(21)). Even though the model suggests less hydrogen production at room temperature, the hydrogen saturation is slower but remains constant (Figure 2.6). These results are consistent with existing laboratory studies that report higher bioH_2 production at ambient or mesophilic temperatures than those reported for thermophilic reactors [39]. In addition, the microbial ecology is more diverse in reactors under mesophilic conditions [40]. Finally, increasing the reactor temperature is directly associated with higher energy consumption and costs.

Other parameters also have an important effect on the mixed liquor solid concentration. For instance, increasing HRT provides more contact time for substrate degradation and biomass growth. However, HRT also determines the membrane flux, which determines the TMP. Only a few laboratory studies report better H_2 yields for HRTs between 8 and 9 h in AnMBRs [41,42]. Thus, finding the ideal HRT for hydrogen production in AnMBRs is a critical aspect that requires further research and consideration. Other factors such as substrate composition, influent COD, and operational conditions also play a role in determining the optimal HRT for efficient hydrogen production in AnMBRs. Therefore, a comprehensive approach is necessary to determine the most suitable operating conditions for maximizing hydrogen production while maintaining membrane performance and minimizing fouling.

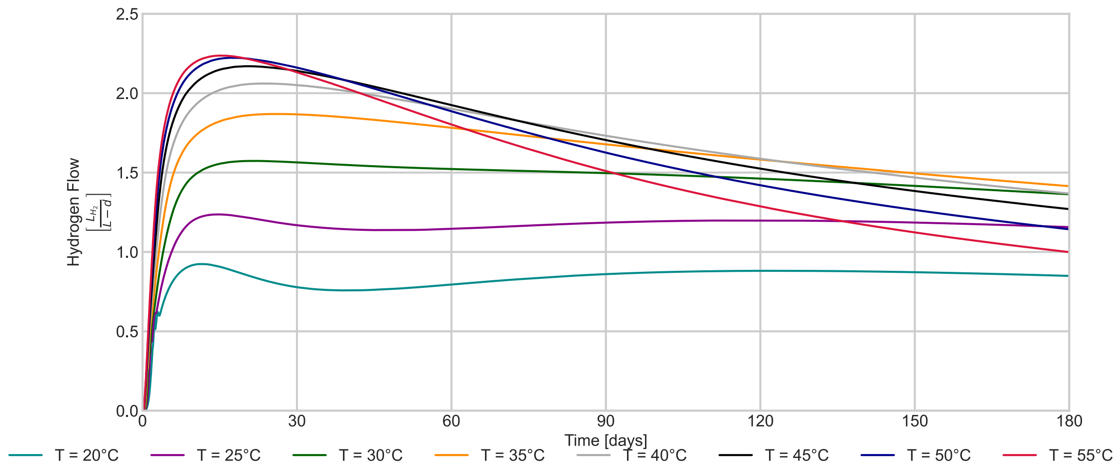

Figura 2.6: Hydrogen rate production at variable temperatures.

The OAT shows that the SRT is a key parameter for bioH_2 production and membrane fouling in an AnMBR. Older biomass might be detrimental to bioH_2 production. Longer SRT reduces the sludge purge, which allows a more concentrated mixed liquor. Higher concentrations of mixed liquor solids increase hydrogen production, affecting EPS concentration and membrane backwashing frequency (Figure 2.4 and Table 2.5).

2.3.4. Model Results for H_2 Production

Table 2.6 shows a comparison between the results of this model and the reported systems for hydrogen production. The existing literature suggests higher hydrogen production rates between 2.5 and 5.8 for submerged AnMBRs using sugar monomers as substrate. Some authors report improved H_2 production in submerged AnMBR by up to 51 % compared to the CSTR without a membrane [43]. By providing additional resistance to the permeate flow, the membrane can act as a degassing mechanism in an AnMBR [7]. However, only a few studies report H_2 productivity while treating complex or multi-substrate effluents. For instance, Lee et al. (2014) [44] reported an H_2 production rate of 10.7 while treating food waste with an inlet COD of 52.7 g/L. Although our study's resulting H_2 production rates are within the production ranges in the existing literature, more information about the substrate composition is required for further validation using reported data. Nevertheless, the developed model in this study serves as a helpful tool to identify operational constraints for H_2 production in AnMBRs.

Tabla 2.6: Comparison among different operational systems for hydrogen production and this study.

Reactor Configuration	**Substrate**	**Inlet COD (gCOD/L)**	**OLR (kg/m^3-d)**	**HTR (h)**	**STR (d)**	**TMP (kPa)**	**Productivity ($L_{H_2}/L-d$)**	**Reference**
External loop	Glucose	10	68 - 92.7	3.3 - 5	2	14	9.2	[45]
External loop	3 Hexoses	20	120 - 480	1 - 4	Unknown	Unknown	66	[31]
Submerged	Glucose	10	26.7	9	450	70	2.5	[46]
Submerged	Glucose	10	40	8	1	Unknown	4.5	[41]
Submerged	Glucose	17	37.5 - 44.3	9	2 - 90	Unknown	5.8	[42]
Submerged	Food waste	52.7	100.2	14	5.37	Unknown	10.7	[44]
Submerged*	Case 1 (protein rich)	10	21.7	12	6	21 - 23	6.1	This study
	Case 2 (sugar rich)						3.8	
	Case 3 (fat rich)						0.7	
	Case 4						5.9	
	Case 5						6.2	
	Case 6						5.8	
	Case 7						6.2	
	Caso 8						5.9	
	Case 9						6.2	
CSRT**	Tofu processing waste	6.3	18.9	8	-	-	8.17	[47]
CSRT**	Cheese whey	60.5	242	6	-	-	2.9	[48]
CSRT**	Lactose	20	80	6	-	-	2.0	[40]

* Content of amino-acids/sugars/fatty-acids/inert-matter composition.
Case 1—100/0/0/0, Case 2—0/100/0/0, Case 3—0/0/100/0, Case 4—30/20/45/5,
Case 5—30/45/20/5, Case 6—31.3/46.3/21.3/0, Case 7—30/45/20/5, Case 8—31.66/31.66/31.66/5,
Case 9—31.66/21.66/46.66/0.
** Studies for H_2 production with raw wastes. No membrane applied.

2.4. Conclusions

We developed a mechanistic model for hydrogen production in a submerged AnMBR. Two aspects differentiate our model from existing literature: First, the model input is a multi-substrate wastewater that includes fractions of proteins, carbohydrates, and lipids. Second, the model integrates the ADM1 model with physical/biochemical processes that affect membrane performance (e.g., membrane fouling). The simulated hydrogen production rates for multi-substrates showed better results than those for mono-substrates (e.g., glucose), specifically when treating amino acids and sugar-rich influents. The highest H_2 production rate for amino acid-rich influents was 6.1 LH_2/L-d; for sugar-rich influents was 5.9 LH_2/L-d; and for lipid-rich influents was 0.7 LH_2/L-d. Modeled membrane fouling and backwashing cycles showed extreme behaviors for amino-acid- and fatty-acid-rich substrates. Finally, mesophilic operation shows promising results for sustaining long-term H_2 production in AnMBR.
The developed model is a valuable tool for the process intensification of H_2 production using fermentative/anaerobic MBR systems; however, further research should include model validation using experimental data. In particular, data from AnMBRs treating multisubstrate effluents are required to optimize the operational conditions for H_2 production.

Author Contributions: G.V.: investigation, conceptualization, methodology, modeling—original code, writing—original draft preparation. F.A.F.: modeling—review and editing, writing—reviewing and editing. A.L.P.: visualization, conceptualization, supervision, funding acquisition, project administration, writing—reviewing and editing. All authors have read and agreed to the published version of the manuscript.

Funding: This research was partially financed by ANID FONDECYT 11191123.

Conflicts of Interest: The authors declare no conflict of interest.

2.5. References

[1] Boese-Cortés, I.; Díaz-Alvarado, F.A.; Prieto, A.L. Biocatalytic membrane reactor modeling for fermentative hydrogen production from wastewater: A review. Int. J. Hydrogen Energy 2023, 48, 13024–13043.

[2] Goveas, L.C.; Nayak, S.; Kumar, P.S.; Vinayagam, R.; Selvaraj, R.; Rangasamy, G. Recent advances in fermentative biohydrogen production. Int. J. Hydrogen Energy. 2023.

[3] Aziz, M.; Darmawan, A.; Juangsa, F.B. Hydrogen production from biomasses and wastes: A technological review. Int. J. Hydrogen Energy 2021, 46, 33756–33781.

[4] Yang,W.; Cicek, N.; Ilg, J. State-of-the-art of membrane bioreactors: Worldwide research and commercial applications in North America. J. Membr. Sci. 2006, 270, 201–211.

[5] Wang, Z.; Wu, Z.; Mai, S.; Yang, C.; Wang, X.; An, Y.; Zhou, Z. Research and applications of membrane bioreactors in China: Progress and prospect. Sep. Purif. Technol. 2008, 62, 249–263.

[6] Zielinska, M.; Ojo, A. Anaerobic membrane bioreactors (ANMBRs) for wastewater treatment: Recovery of nutrients and energy, and management of fouling. Energies 2023, 16, 2829.

[7] Prieto, A.L.; Sigtermans, L.H.; Mutlu, B.R.; Aksan, A.; Arnold, W.A.; Novak, P.J. Performance of a composite bioactive membrane for H2 production and capture from high strength wastewater. Environ. Sci. Water Res. Technol. 2016, 2, 848–857.

[8] Kong, Z.; Li, L.; Wu, J.; Wang, T.; Rong, C.; Luo, Z.; Pan, Y.; Li, D.; Li, Y.; Huang, Y.; et al. Evaluation of bio-energy recovery from the anaerobic treatment of municipal wastewater by a pilot-scale submerged anaerobic membrane bioreactor (AnMBR) at ambient temperature. Bioresour. Technol. 2021, 339, 125551.

[9] Zhang, M.-L.; Fan, Y.-T.; Xing, Y.; Pan, C.-M.; Zhang, G.-S.; Lay, J.-J. Enhanced biohydrogen production from cornstalk wastes with acidification pretreatment by mixed anaerobic cultures. Biomass-Bioenergy 2007, 31, 250–254.

[10] Karlsson, A.; Vallin, L.; Ejlertsson, J. Effects of temperature, hydraulic retention time and hydrogen extraction rate on hydrogen production from the fermentation of food industry residues and manure. Int. J. Hydrogen Energy 2008, 33, 953–962.

[11] Ren, N.; Wang, A.; Cao, G.; Xu, J.; Gao, L. Bioconversion of lignocellulosic biomass to hydrogen: Potential and challenges. Biotechnol. Adv. 2009, 27, 1051–1060.

[12] Ahmad, T.; Aadil, R.M.; Ahmed, H.; Rahman, U.U.; Soares, B.C.; Souza, S.L.; Pimentel, T.C.; Scudino, H.; Guimarães, J.T.; Esmerino, E.A.; et al. Treatment and utilization of dairy industrial waste: A review. Trends Food Sci. Technol. 2019, 88, 361–372.

[13] Panigrahi, S.; Dubey, B.K. A critical review on operating parameters and strategies to improve the biogas yield from anaerobic digestion of organic fraction of municipal solid waste. Renew. Energy 2019, 143, 779–797.

[14] Banu, J.R.; Usman, T.M.; Kavitha, S.; Yukesh Kannah, R.; Yogalakshmi, K.N.; Sivashanmugam, P.; Bhatnagar, A.; Kumar, G. A critical review on limitations and enhancement strategies associated with biohydrogen production. Int. J. Hydrogen Energy 2021, 46, 16565–16590.

[15] Batstone, D.J.; Keller, J.; Angelidaki, I.; Kalyuzhnyi, S.V.; Pavlostathis, S.G.; Rozzi, A.; Sanders, W.T.M.; Siegrist, H.A.; Vavilin, V.A. The IWA Anaerobic Digestion Model No 1 (ADM1). Water Sci. Technol. 2002, 45, 65–73.

[16] Shin, C.; Tilmans, S.H.; Chen, F.; Criddle, C.S. Anaerobic membrane bioreactor model for design and prediction of domestic wastewater treatment process performance. Chem. Eng. J. 2021, 426, 131912.

[17] Siegrist, H.; Vogt, D.; Garcia-Heras, J.L.; Gujer, W. Mathematical model for meso- and thermophilic anaerobic sewage sludge digestion. Environ. Sci. Technol. 2002, 36, 1113–1123.

[18] Chen, R.; Nie, Y.; Hu, Y.; Miao, R.; Utashiro, T.; Li, Q.; Xu, M.; Li, Y.-Y. Fouling behaviour of soluble microbial products and extracellular polymeric substances in a submerged anaerobic membrane bioreactor treating low-strength wastewater at room temperature. J. Membr. Sci. 2017, 531, 1–9.

[19] Maaz, M.; Yasin, M.; Aslam, M.; Kumar, G.; Atabani, A.; Idrees, M.; Anjum, F.; Jamil, F.; Ahmad, R.; Khan, A.L.; et al. Anaerobic membrane bioreactors for wastewater treatment: Novel configurations, fouling control and energy considerations. Bioresour. Technol. 2019, 283, 358–372.

[20] Jang, N.; Ren, X.; Cho, J.; Kim, I.S. Steady-state modeling of bio-fouling potentials with respect to the biological kinetics in the submerged membrane bioreactor (SMBR). J. Membr. Sci. 2006, 284, 352–360.

[21] Gautam, R.K.; Kamilya, T.; Verma, S.; Muthukumaran, S.; Jegatheesan, V.; Navaratna, D. Evaluation of membrane cake fouling mechanism to estimate design parameters of a submerged AnMBR treating high strength industrial wastewater. J. Environ. Manag. 2022, 301, 113867.

[22] Hosseinzadeh, A.; Zhou, J.L.; Altaee, A.; Li, D. Machine learning modeling and analysis of biohydrogen production from wastewater by dark fermentation process. Bioresour. Technol. 2022, 343, 126111.

[23] Li, G.; Ji, J.; Ni, J.; Wang, S.; Guo, Y.; Hu, Y.; Liu, S.; Huang, S.-F.; Li, Y.-Y. Application of deep learning for predicting the treatment performance of real municipal wastewater based on one-year operation of two anaerobic membrane bioreactors. Sci. Total Environ. 2022, 813, 151920.

[24] Yao, J.;Wu, Z.; Liu, Y.; Zheng, X.; Zhang, H.; Dong, R.; Qiao,W. Predicting membrane fouling in a high solid AnMBR treating OFMSW leachate through a genetic algorithm and the optimization of a BP neural network model. J. Environ. Manag. 2022, 307, 114585.

[25] Nagaoka, S.H.; Ueda, A.M. Influence of bacterial extracellular polymers on the membrane separation activated sludge process. Water Sci. Technol. 1996, 34, 165–172.

[26] Kunatsa, T.; Xia, X. A review on anaerobic digestion with focus on the role of biomass co-digestion, modelling and optimisation on biogas production and enhancement. Bioresour. Technol. 2022, 344, 126311.

[27] Etuwe, C.N.; Momoh, Y.O.L.; Iyagba, E.T. Development of Mathematical Models and Application of the Modified Gompertz Model for Designing Batch Biogas Reactors. Waste Biomass-Valorization 2016, 7, 543–550.

[28] Taheri, E.; Amin, M.M.; Fatehizadeh, A.; Rezakazemi, M.; Aminabhavi, T.M. Artificial intelligence modeling to predict transmembrane pressure in anaerobic membrane bioreactor-sequencing batch reactor during biohydrogen production. J. Environ. Manag. 2021, 292, 112759.

[29] Ashok, M.; Kumar, M. Anaerobic Membrane Reactors for Biohydrogen Production; Elsevier: Amsterdam, The Netherlands, 2020; pp. 367–397.

[30] Ngo, H.H.; Khan, M.A.; Guo, W.; Liu, Y.; Zhang, X.; Li, J.; Wang, J. Energy Production in Anaerobic Membrane Bioreactors: Opportunities and Challenges; Elsevier: Amsterdam, The Netherlands, 2020; pp. 309–333.

[31] Lee, K.-S.; Lin, P.-J.; Fangchiang, K.; Chang, J.-S. Continuous hydrogen production by anaerobic mixed microflora using a hollow-fiber microfiltration membrane bioreactor. Int. J. Hydrogen Energy 2007, 32, 950–957.

[32] Yoon, S.-H. Membrane Bioreactor Processes; CRC Press: Boca Raton, FL, USA, 2015.

[33] Navaratna, D.; Shu, L.; Baskaran, K.; Jegatheesan, V. Model development and parameter estimation for a hybrid submerged membrane bioreactor treating Ametryn. Bioresour. Technol. 2012, 113, 191–200.

[34] Ran, N.; Sharon-Gojman, R.; Larsson, S.; Gillor, O.; Mauter, M.S.; Herzberg, M. Unraveling pH Effects on Ultrafiltration Membrane Fouling by Extracellular Polymeric Substances: Adsorption and Conformation Analyzed with Localized Surface Plasmon Resonance. Environ. Sci. Technol. 2022, 56, 14763–14773.

[35] Wang, Z.; Wu, Z.; Tang, S. Extracellular polymeric substances (EPS) properties and their effects on membrane fouling in a submerged membrane bioreactor. Water Res. 2009, 43, 2504–2512.

[36] Lew, B.; Tarre, S.; Beliavski, M.; Dosoretz, C.; Green, M. Anaerobic membrane bioreactor (AnMBR) for domestic wastewater treatment. Desalination 2009, 243, 251–257.

[37] Ozgun, H.; Dereli, R.K.; Ersahin, M.E.; Kinaci, C.; Spanjers, H.; van Lier, J.B. A review of anaerobic membrane bioreactors for municipal wastewater treatment: Integration options, limitations and expectations. Sep. Purif. Technol. 2013, 118, 89–104.

[38] Nilusha, R.T.; Wang, T.; Wang, H.; Yu, D.; Zhang, J.; Wei, Y. Optimization of in situ backwashing frequency for stable operation of anaerobic ceramic membrane bioreactor. Processes 2020, 8, 545.

[39] Qiu, C.; Zheng, Y.; Zheng, J.; Liu, Y.; Xie, C.; Sun, L. Mesophilic and Thermophilic Biohydrogen Production from Xylose at Various Initial pH and Substrate Concentrations with Microflora Community Analysis. Energy Fuels 2016, 30, 1113–1123.

[40] Qin, Y.; Cheng, H.; Li, Y.-Y. Sustainable anaerobic technologies for biogas and biohythane production. In Biomass, Biofuels, Biochemicals: Circular Bioe-Conomy: Technologies for Waste Remediation; Elsevier: Amsterdam, The Netherlands, 2022.

[41] Shen, L.; Bagley, D.M.; Liss, S.N. Effect of organic loading rate on fermentative hydrogen production from continuous stirred tank and membrane bioreactors. Int. J. Hydrogen Energy 2009, 34, 3689–3696.

[42] Lee, D.-Y.; Li, Y.-Y.; Noike, T. Influence of solids retention time on continuous H2 production using membrane bioreactor. Int. J. Hydrogen Energy 2010, 35, 52–60.

[43] Noblecourt, A.; Christophe, G.; Larroche, C.; Santa-Catalina, G.; Trably, E.; Fontanille, P. High hydrogen production rate in a submerged membrane anaerobic bioreactor. Int. J. Hydrogen Energy 2017, 42, 24656–24666.

[44] Lee, D.; Xu, K.; Kobayashi, T.; Li, Y.; Inamori, Y. Effect of organic loading rate on continuous hydrogen production from food waste in submerged anaerobic membrane bioreactor. Int. J. Hydrogen Energy 2014, 39, 16863–16871.

[45] Oh, S.-E.; Iyer, P.; Bruns, M.A.; Logan, B.E. Biological hydrogen production using a membrane bioreactor. Biotechnol. Bioeng. 2004, 87, 119–127.

[46] Lee, D.-Y.; Li, Y.-Y.; Noike, T.; Cha, G.-C. Behavior of extracellular polymers and bio-fouling during hydrogen fermentation with a membrane bioreactor. J. Membr. Sci. 2008, 322, 13–18.

[47] Kim, D.; Lee, D.; Kim, M. Enhanced biohydrogen production from tofu residue by acid/base pretreatment and sewage sludge addition. Int. J. Hydrogen Energy 2011, 36, 13922–13927.

[48] Venetsaneas, N.; Antonopoulou, G.; Stamatelatou, K.; Kornaros, M.; Lyberatos, G. Using cheese whey for hydrogen and methane generation in a two-stage continuous process with alternative pH controlling approaches. Bioresour. Technol. 2009, 100, 3713–3717.

[49] Palomo-Briones, R.; Razo-Flores, E.; Bernet, N.; Trably, E. Dark-fermentative biohydrogen pathways and microbial networks in continuous stirred tank reactors: Novel insights on their control. Appl. Energy 2017, 198, 77–87.

Capítulo 3

Conclusions

In this master thesis a mechanistic model for hydrogen production in a submerged AnMBR. Two aspects differentiate this model from existing literature: in the first place, the model input is a multi-substrate wastewater that includes fractions of proteins, carbohydrates, and lipids; which corresponds to a novelty compared to monosubstrate models. In the second place, the model integrates physical/biochemical processes that affect membrane performance (e.g., membrane fouling). The simulated hydrogen production rates for multi-substrates showed better results than those for mono-substrates (e.g., glucose), specifically when treating amino acids and sugar-rich influents. The highest H_2 production rate for amino acid-rich influents was 6.1 LH_2/L-d; for sugar-rich influents was 5.9 LH_2/L-d; and for lipid-rich influents was 0.7 LH_2/L-d. Modeled membrane fouling and backwashing cycles showed extreme behaviors for amino-acid- and fatty-acid-rich substrates. Finally, mesophilic operation shows promising results for sustaining long-term H_2 production in AnMBR.

The developed model is a valuable tool for the process intensification of H_2 production using fermentative/anaerobic MBR systems; however, further research should include model validation using experimental data. In particular, data from AnMBRs treating multisubstrate effluents are required to optimize the operational conditions for H_2 production, and for systems design.

Bibliografía

Aziz, M., y cols. (2021). Hydrogen production from biomasses and wastes: A technological review. *International Journal of Hydrogen Energy*, *46*(68), 33756-33781. doi: https://doi.org/10.1016/j.ijhydene.2021.07.189

Batstone, D., Keller, J., Angelidaki, I., Kalyuzhnyi, S., Pavlostathis, S., Rozzi, A., ... Vavilin, V. (2002, 02). Anaerobic digestion model no 1 (adm1). *Water science and technology : a journal of the International Association on Water Pollution Research*, *45*, 65-73.

Boese-Cortés, I., y cols. (2023). Biocatalytic membrane reactor modeling for fermentative hydrogen production from wastewater: A review. *International Journal of Hydrogen Energy*, *48*(35), 13024-13043. doi: https://doi.org/10.1016/j.ijhydene.2022.12.188

Chen, R., Nie, Y., Hu, Y., Miao, R., Utashiro, T., Li, Q., ... Li, Y.-Y. (2017). Fouling behaviour of soluble microbial products and extracellular polymeric substances in a submerged anaerobic membrane bioreactor treating low-strength wastewater at room temperature. *Journal of Membrane Science*, *531*, 1-9. doi: https://doi.org/10.1016/j.memsci.2017.02.046

García-Depraect, O., Valdez-Vázquez, I., Rene, E. R., Gómez-Romero, J., López-López, A., y León-Becerril, E. (2019). Lactate- and acetate-based biohydrogen production through dark co-fermentation of tequila vinasse and nixtamalization wastewater: Metabolic and microbial community dynamics. *Bioresource Technology*, *282*, 236-244. doi: https://doi.org/10.1016/j.biortech.2019.02.100

Gautam, R. K., y cols. (2022). Evaluation of membrane cake fouling mechanism to estimate design parameters of a submerged anmbr treating high strength industrial wastewater. *Journal of Environmental Management*, *301*, 113867. doi: https://doi.org/10.1016/j.jenvman.2021.113867

Hawkes, F. R., y cols. (2007). Continuous dark fermentative hydrogen production by mesophilic microflora: Principles and progress. *International Journal of Hydrogen Energy*, *32*(2), 172-184. doi: https://doi.org/10.1016/j.ijhydene.2006.08.014

Jang, N., y cols. (2006). Steady-state modeling of bio-fouling potentials with respect to the biological kinetics in the submerged membrane bioreactor (smbr). *Journal of Membrane Science*, *284*(1), 352-360. doi: https://doi.org/10.1016/j.memsci.2006.08.001

Kapdan, I. K., y Kargi, F. (2006). Bio-hydrogen production from waste materials. *Enzyme and Microbial Technology*, *38*(5), 569-582. doi: https://doi.org/10.1016/j.enzmictec.2005.09.015

Maaz, M., Yasin, M., Aslam, M., Kumar, G., Atabani, A., Idrees, M., … Kim, J. (2019). Anaerobic membrane bioreactors for wastewater treatment: Novel configurations, fouling control and energy considerations. *Bioresource Technology*, *283*, 358-372. doi: https://doi.org/10.1016/j.biortech.2019.03.061

Meher Kotay, S., y Das, D. (2008). Biohydrogen as a renewable energy resource—prospects and potentials. *International Journal of Hydrogen Energy*, *33*(1), 258-263. (IWHE 2006) doi: https://doi.org/10.1016/j.ijhydene.2007.07.031

Prieto, A. L., Sigtermans, L. H., Mutlu, B. R., Aksan, A., Arnold, W. A., y Novak, P. J. (2016). Performance of a composite bioactive membrane for h2 production and capture from high strength wastewater. *Environ. Sci.: Water Res. Technol.*, *2*, 848-857. doi: 10.1039/C6EW00101G

Rahman, S., Masdar, M., Rosli, M., Majlan, E., Husaini, T., Kamarudin, S., y Daud, W. (2016). Overview biohydrogen technologies and application in fuel cell technology. *Renewable and Sustainable Energy Reviews*, *66*, 137-162. doi: https://doi.org/10.1016/j.rser.2016.07.047

Ramos, L. R., y Silva, E. L. (2018). Continuous hydrogen production from cofermentation of sugarcane vinasse and cheese whey in a thermophilic anaerobic fluidized bed reactor. *International Journal of Hydrogen Energy*, *43*(29), 13081-13089. doi: https://doi.org/10.1016/j.ijhydene.2018.05.070

Shin, C., y cols. (2021). Anaerobic membrane bioreactor model for design and prediction of domestic wastewater treatment process performance. *Chemical Engineering Journal*, *426*, 131912. doi: https://doi.org/10.1016/j.cej.2021.131912

Siegrist, H., y cols. (2002). Mathematical model for meso- and thermophilic anaerobic sewage sludge digestion. *Environmental Science & Technology*, *36*(5), 1113-1123. (PMID: 11917999) doi: 10.1021/es010139p

Vera, G., Feijoo, F. A., y Prieto, A. L. (2023). A mechanistic model for hydrogen production in an anmbr treating high strength wastewater. *Membranes*, *13*(11). doi: 10.3390/membranes13110852